

EVALUATION OF BIOMECHANICAL BEHAVIOR OF MAXILLARY INCISORS BY VARYING THE NON-CARIOUS CERVICAL LESION MORPHOLOGY, LOAD TYPE AND COMPOSITE RESIN RESTORATION: A 3D FINITE ELEMENT STUDY

Daniela Navarro Ribeiro Teixeira – Faculdade de Odontologia da Universidade Federal de Uberlândia – dnrteixeira@gmail.com

Marina Ferreira de Lima Naves – Faculdade de Odontologia da Universidade Federal de Uberlândia – marinalimanaves@gmail.com

Lívia Fávaro Zeola – Faculdade de Odontologia da Universidade Federal de Uberlândia – liviazeola@gmail.com

Alexandre Coelho Machado – Faculdade de Odontologia da Universidade Federal de Uberlândia – alexandrecoelhomachado@gmail.com

Paulo Vinícius Soares – Faculdade de Odontologia da Universidade Federal de Uberlândia – paulovsoares@yahoo.com.br

Abstract. *Non-carious cervical lesions (NCCLs) are formed by loss of tooth structure in the cervical third of the crown and root surface, with multi-factorial origin. The aim of this study was to measure the effect of five morphological types of NCCLs, simulating two different loads on maxillary incisors, by quantifying the stress distributions. Eleven virtual models of maxillary incisors were generated using the CAD software through of tooth 21 sound. These models presented six NCCLs morphologies: Sound (H), CONCAVE (CO), IRREGULAR (IR), NOTCHED (NO), SHALLOW (SH) AND WEDGED-SHAPE (WS); unrestored and restored with composite resin. The models were exported to an analyses software (Ansys Workbench 12.0), considered homogeneous, linear and isotropic. Then, the models were meshed and submitted to two types of load (500 MPa): (ML)- Palatine Middle Third and (IL)- Palatine Incisal Third. The displacement restriction was made on the base and on the sides of the bone. Data summarizing the stress distributions were obtained in MPa using Von Mises criteria. As results, the models CO, WS and IR showed higher stress concentration on the bottom of the lesion. Models with the center of the NCCL at acute angle (WS and IR) showed higher stress on the junction of the ceiling and floor walls. All the restored morphologies, independent of the load type, showed biomechanical behavior similar to the H. It was conclude that deeper NCCLs and with acute angles, shows higher stress on the deep of the lesion; and restore with composite resin is important, independent of the morphology.*

Key-words: *Biomechanical Behavior, Composite Resin Restoration, Dental Wear, Finite Element Analysis, Non-carious cervical lesions.*

1. INTRODUCTION

The morphology of the dentition is considered central to many areas of study (Guatelli-Steinberg et al., 2005), especially when it comes to the shape of the crown and root, and tooth wear processes (Benazzi et al., 2013; Soares et al., 2014). The anatomy of the tooth crown is influenced by the process of evolution of the species to better adaptation to their habits, such as chewing efficiency (Benazzi et al., 2013). Thus, although the variation in the occlusal topography which improves the masticatory efficiency, there are morphological characteristics acquired which can promote dental biomechanical damage to the tooth, such as non-carious cervical lesions (NCCLs) (Soares et al., 2014).

The NCCLs are defects formed by loss of tooth structure in the cervical area of the crown, reaching the root surface (Michael et al., 2009). There are three principal factors that explain the origin and progression of the NCCLs: biocorrosion, friction and stress (Grippio et al., 2012). They can be classified as shallow, notched, concave, wedge-shaped and irregular geometry, when it comes to anterior teeth (Michael et al., 2010). There are a variety of restorative materials that can be used for its treatment: glass ionomer cement, resin-modified glass ionomer, flowable composite resins and nano hybrid composite resins (Perez, 2010; Ferracane, 2011).

Thus, the purpose of this study was to simulate the influence of an adhesive restoration, such as a hybrid composite resin, and two types of load application on maxillary incisors with five different NCCLs morphologies, by analyzing the stress distribution patterns, using three-dimensional (3D) finite element analysis (FEA).

2. METHODS AND MATERIALS

3D linear elastic analysis was performed using anatomically-based geometric representations for the dentin, pulp, enamel, periodontal ligament, cortical and trabecular bone. Beyond the Sound model (SO), It was simulated five NCCL morphologies: Shallow type (SH), Notched (NO), Concave (CO), Wedged-shape (WS) and Irregular geometry (IR'-

WS) (IR^o- CO) – sharp internal line angle; and IR^o(CO) – rounded internal line angle) (Michael et al., 2010). (Figure 1).

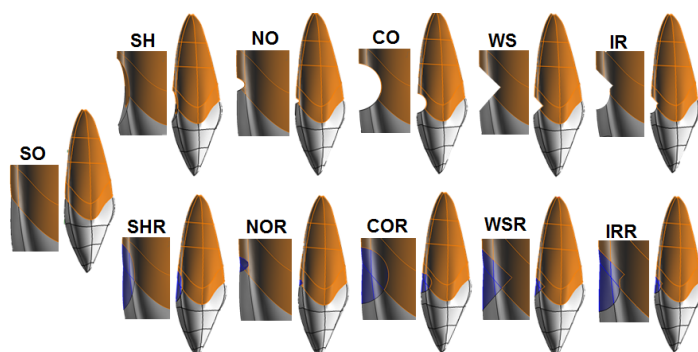


Figure 1. Anterior NCCLs morphologies and respective restorations simulated models.

The models were exported using the STEP format (Fig. 1) to the processing analysis software (ANSYS 12.0, Ansys Workbench 12.0.1, Canonsburg, PA, EUA). The following steps were performed in this software: pre-processing (definition of mechanical properties, volumes, connection types, mesh for each structure, and boundary conditions), processing (data calculation) and post-processing (analysis of results by stress distribution criteria). All dental structures and restorative materials were considered homogeneous and linear elastic. Enamel and dentin were considered orthotropic and the other structures isotropic (Table 1) (Carter et al., 1977; Weinstein et al., 1980; Rubin et al., 1983; Shinya et al., 2008; Miura et al., 2009).

Table 1 Mechanical properties used to perform orthotropic and isotropic structures.

Structures	Orthotropic Structures			Reference
	Elastic Modulus (MPa)			
	LONGITUDINAL	TRANSVERSAL	Z	Miura et al., 2009
Enamel	73720	63270	63270	
Dentin	17070	5610	5610	
	Shear coefficient (MPa)			
Enamel	20890	24070	20890	
Dentin	1700	6000	1700	
	Poisson Ratio (ν)			
Enamel	0.23	0.45	0.23	
Dentin	0.30	0.33	0.30	
Structures	Isotropic Structures			
	Elastic Modulus (MPa)		Poisson Ratio (ν)	
Pulp	2.07		0.45	Rubin et al., 1983
Periodontal Ligament	68.9		0.45	Weinstein et al., 1980
Cortical Bone	13,700		0.30	Carter et al., 1977
Medular Bone	1,370		0.30	Carter et al., 1977
Hybrid Composite Resin	22,000		0.27	Shinya et al., 2008

After testing the mesh conversion to define the appropriate mesh refinement level, volumes corresponding to each structure were meshed with the controlled and connected elements. The meshing process involved division of the studied system into a set of small discrete elements defined by nodes. Solid quadratic tetrahedral elements of 10 nodes were used (Fig. 2A). The mesh conversion test was initiated using the software automatic meshing and was continued by gradually decreasing the size of the elements. For each test stage, the results were generated by equivalent stress criterion (von Mises) to verify the higher stress values on dentin. The mesh was considered satisfactory when, even reducing the dimension of elements, the higher stress levels were similar to the results observed with the previous mesh refinement. The number of elements used varied depending on the different volumes, so that the final model accurately

represented the original geometry. Due to the adhesive properties of the restorative materials used, restorations were bonded to dental structures by considering a mesh connection with dentin and enamel.

The boundary conditions consisted of developing a displacement/restriction model using load application. Loading of models (500 N) (Poiate et al., 2009) was applied to specific surfaces previously defined in the CAD software, as follows: (ML) - Palatine Middle Third and (IL)- Palatine Incisal Third. These loads simulated non-physiologic occlusal forces on incisor palatal movements, during the anterior guidance (Schuyler, 2001). ML was considered the beginning and IL the end of this movement. Models were restrained at the base and lateral surfaces of cortical and trabecular bone to avoid displacement (Figure 2). The stress distribution analyses were calculated using the Maximum Principal Stress, measured in MPa. Two specific regions, were selected for stress measurement in each NCCL: bottom of the lesion (BW) and the pulp/dentin interface wall (IW). For the IR morphology, were selected two points for each bottom of the lesion. After complete stress analysis in all structures, the results were plotted in transparency, except for enamel, dentin and restorative materials, for better visualization.

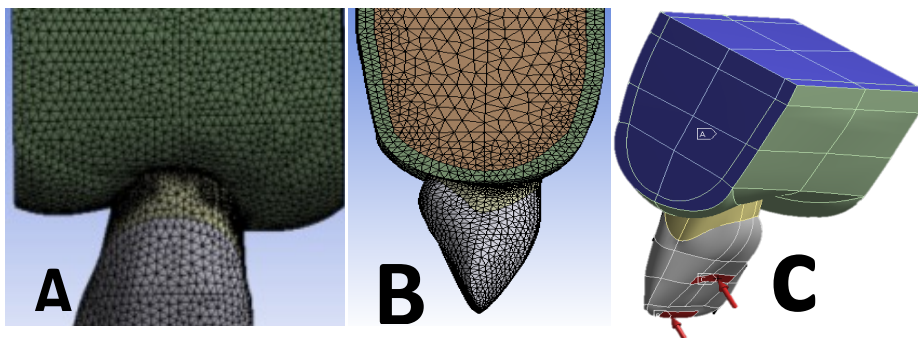


Figure 2. Mesh of the healthy upper central incisor: A) Frontal view; B) Lateral view. Boundary Conditions: C) The red arrows represent the two types of applied load (500N): ML - Palatine Middle Third and IL- Palatine Incisal Third, and the blue area represents the restrained models at the base and lateral surfaces of cortical and trabecular bone to avoid displacement.

3. RESULTS

The maximum principal stress (σ_1) distribution between all the models under different loading conditions is shown in Figs. 3, 4, 5 and 6. Positive and negative values indicate that the corresponding regions are subjected to tensile or compressive stresses, respectively.

The NO, WS and IR' (WS) models demonstrated higher compressive stress concentration on the bottom of the lesion, for both load types. On the other hand, SH, CO and IR''(CO) presented more harmonic stress distribution pattern (Figs 3, 4, 5, and 6).

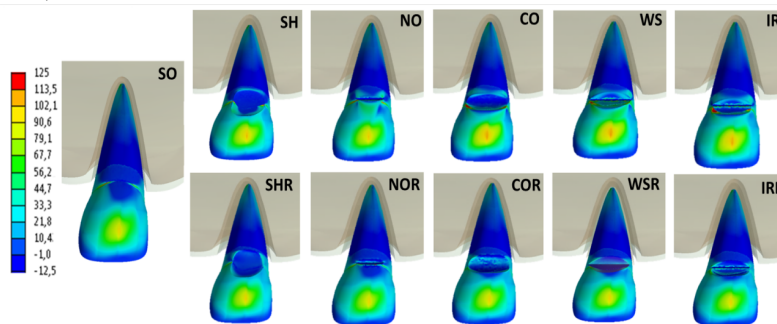


Figure 3. Maximum Principal Stress (MPa) distribution for models that received Palatine Middle Third (ML).

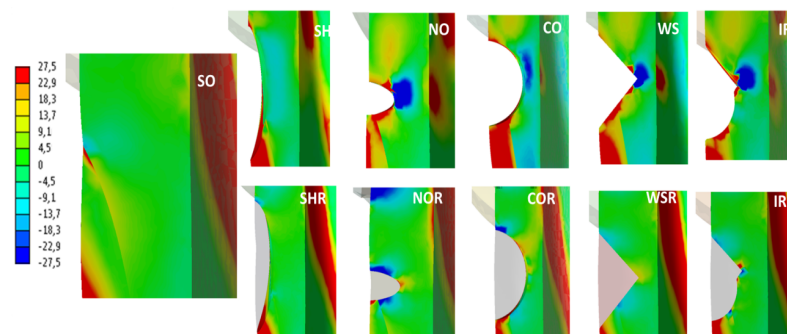


Figure 4. Maximum Principal Stress (MPa) distribution on NCCLs morphologies areas on models that received ML.

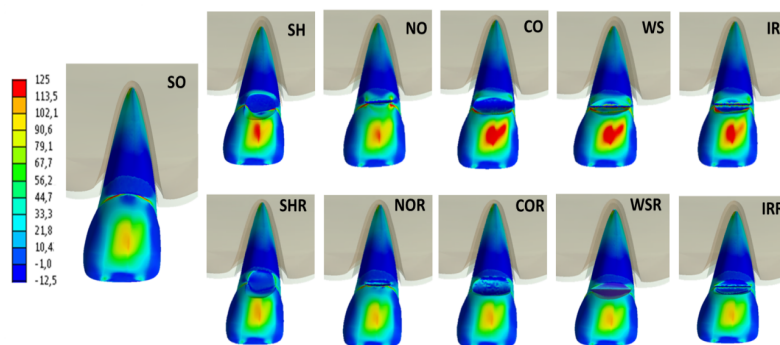


Figure 5. Maximum Principal Stress (MPa) distribution for models that received Palatine Incisal Third (IL).

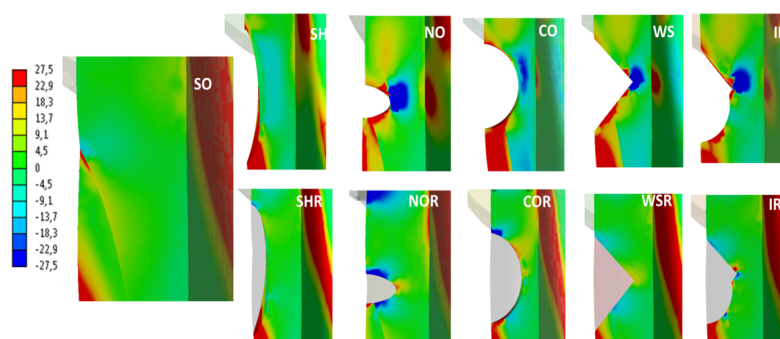


Figure 6. Maximum Principal Stress (MPa) distribution on NCCLs morphologies areas on models that received IL.

For all the morphologies, the IL was associated with more compressive stress concentration on bottom of the lesions than ML, even as tensile stresses on pulp-dentin interface (Figs 4 and 6). For IL, the morphologies SH and CO demonstrated tensile stress concentration on enamel area, where as WS presented tensile stress on dentin, at the upper and lower walls. IR and NO demonstrated tensile stress concentration on enamel and dentin (Figure 5).

The sound teeth demonstrated lower compressive stress (-8,83MPa) compared to sharp angle morphologies, beyond NO (-46,97MPa). The higher compressive stress was found on WS morphology (-109,2MPa) and on IR'(WS) geometry (-91,28MPa). On IW, the morphologies presented tensile stress concentration, with exception of CO (0,92 MPa) and IR''(CO) (-0,73 MPa), which demonstrated compressive stress values. The higher tensile stress concentration was found on NO geometry (16,85 MPa), following by SH (11,71MPa), IR'(WS) (11,12 MPa) and WS (10,9 MPa) (Figure 7).

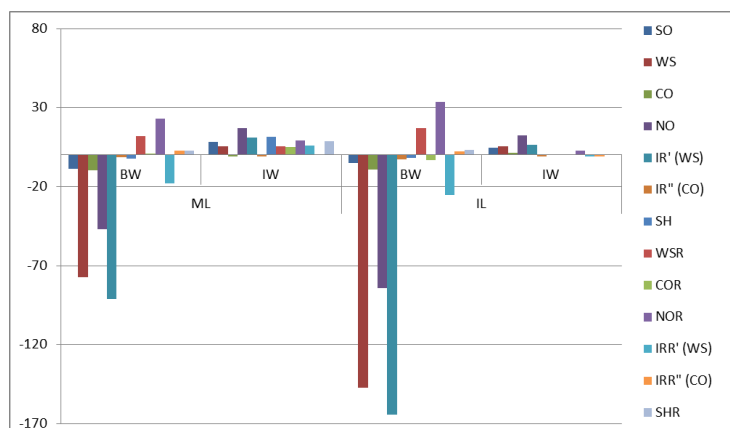


Figure 7. Maximum Principal Stress values (MPa) on NCCLs at specific regions on models: BW and IW.

For IL, it was not found tensile stress on BW. The geometries WS (-204,3 MPa), IR' (-164,21 MPa) and NO (-84,36 MPa), demonstrated as results higher values of compression compared to ML. On IW, the WS morphology presented the greater tensile stress concentration (12,73 MPa), followed by NO (12,4 MPa) (Figure 7).

The simulated hybrid composite resin restoration promoted more harmonic biomechanical behavior for all morphologies, independent of load type. However, the models with restored with composite resin expressed different magnitude of stress on BL, mainly for NOR, which presented tensile stress, and IR'R(WS), that showed compressive stress. For IL, analyzing the BL, the higher compressive stress was found on IR'R(WS) morphology (-25,27 MPa), and the higher tensile stress was found on NOR morphology (33,75 MPa). For ML, the higher tensile stress was found on NOR morphology (23 MPa), analyzing the bottom dentin, and the higher compressive stress was found on IR'(WS) morphology (-18,03 MPa) (Figure 7).

4. REFERENCES

Benazzi S, Nguyen HN, Kullmer O, Hublin JJ. 2013. Unravelling the functional biomechanics of dental features and tooth wear. *PLoS One* 8: e69990.

Carter DR, Hayes WC (1977) The compressive behavior of bone as a two-phase porous structure. *J Bone Joint Surg Am* 59: 954-962.

Ferracane JL. 2011. Resin composite--state of the art. *Dent Mater* 27: 29-38.

Grippo, J.O., Simring, M. & Coleman, T.A. 2012. "Abfraction, abrasion, biocorrosion, and the enigma of noncarious cervical lesions: a 20-year perspective". *J Est Rest Dent*, 24(1) 10-23.

Guatelli-Steinberg D, Reid DJ, Bishop TA, Larsen CS. 2005. Anterior tooth growth periods in Neandertals were comparable to those of modern humans. *Proc Natl Acad Sci USA*, 102: 14197-202.

Michael JA, Kaidonis JA, Townsend GC. 2010. Non-carious cervical lesions on permanent anterior teeth: a new morphological classification. *Aust Dent J* 55: 134-137.

Michael JA, Townsend GC, Greenwood LF, Kaidonis JA. 2009. Abfraction: separating fact from fiction. *Aust Dent J* 54: 2-8.

Miura J, Maeda Y, Nakai H, Zako M. 2009. Multiscale analysis of stress distribution in teeth under applied forces. *Dent Mater* 25: 67-73.

Perez CR. 2010. Alternative technique for class V resin composite restorations with minimum finishing/polishing procedures. *Oper Dent* 35: 375-379.

Poiate IA, de Vasconcellos AB, de Santana RB, Poiate E. 2009. Three-dimensional stress distribution in the human periodontal ligament in masticatory, parafunctional, and trauma loads: finite element analysis. *J Periodontol* 80: 1859-1867.

Rubin C, Krishnamurthy N, Capilouto E, Yi H (1983) Stress analysis of the human tooth using a three-dimensional finite element model. *J Dent Res* 62: 82-86.

Schuyler CH. 2001. The function and importance of incisal guidance in oral rehabilitation. 1963. *J Prosthet Dent* 86: 219-232.

Shinya A, Yokoyama D, Lassila LV, Vallittu PK. 2008. Three-dimensional finite element analysis of metal and FRC adhesive fixed dental prostheses. *J Adhes Dent* 10: 365-371.

Soares PV, Souza LV, Verissimo C, Zeola LF, Pereira AG, et al. 2014. Effect of root morphology on biomechanical behaviour of premolars associated with abfraction lesions and different loading types. *J Oral Rehabil* 41: 108-114.

Weinstein AM, Klawitter JJ, Cook SD (1980) Implant-bone interface characteristics of bioglass dental implants. *J Biomed Mater Res* 14: 23-29.

5. ACKNOWLEDGMENTS

The authors would like to thank the Integrated Dental Research Laboratory of the Federal University of Uberlândia (CPBio) for the structure to perform the finite element analysis.

6. ACCOUNTABILITY OF INFORMATION

All the authors are responsible for the information include on this paper.